Article

Adipose Stem Cell Response to Borophosphate Bioactive Glass

Nada A. Abokefa [1,†], Bradley A. Bromet [1,†], Rebekah L. Blatt [2], Makenna S. Pickett [1], Richard K. Brow [2] and Julie A. Semon [1,*]

1 Department of Biological Sciences, Missouri University of Science and Technology, Rolla, MO 65409, USA; naa8nn@mst.edu (N.A.A.); babn83@mst.edu (B.A.B.)
2 Department of Materials Science and Engineering, Missouri University of Science and Technology, Rolla, MO 65409, USA; brow@mst.edu (R.K.B.)
* Correspondence: semonja@mst.edu
† These authors contributed equally to this work.

Abstract: Silicate and borate bioactive glasses have been reported to create alkaline conditions by rapidly releasing ions when reacting in aqueous solution. At certain levels, this alkaline solution can negatively affect cell viability. Adding phosphate ions to the glass composition can control the degradation rate of bioactive glasses and create a neutral pH environment. This study evaluated a series of borophosphate bioactive glasses (BPBGs) with nominal molar compositions $16Na_2O-24CaO-xB_2O_3-(60-x)P_2O_5$, where $x = 0$, 40, or 60. The phosphate (X0) glass (PBG) produced an acidic solution when dissolved in water; the borate (X60) glass (BBG) produced an alkaline solution, and the BPBG glass produced a pH-neutral solution. These three glasses were evaluated using adipose stem cells (ASCs), a cell population known for their therapeutic abilities. The effects of each glass on the pH of cell culture, ions released during degradation, and on ASC functions, including viability, migration, angiogenic ability, differentiation, and protein secretions, were evaluated. The X40 BPBG created a physiologically neutral pH in cell culture media after 24 h. The X0 phosphate glass promoted ASC migration, while the highly alkaline X60 borate increased the angiogenic ability of ASCs. These results indicate that BPBG can be used safely in cell culture studies and customized for specific biomedical applications.

Keywords: adipose stem cells; ASCs; borophosphate; bioactive glass

1. Introduction

Bioactive glasses (BGs) are a class of oxide-based ceramics invented by Larry Hench in the late 1960s [1]. BGs have gained interest due to their bioactivity, biocompatibility, ability to bond to hard and soft tissues, and potential to stimulate tissue regeneration [2–4]. They are versatile and can be manufactured in different shapes and sizes, such as powders, fibers, and scaffolds [3,5,6]. Consequently, several BG families have emerged with different compositions, including borate BGs (BBGs). When compared to the traditional silicate BG, BBGs generally have faster degradation rates [7–9], enhanced cell proliferation and differentiation in vitro [10], and tissue infiltration in vivo [11]. BBGs have been shown to help heal chronic wounds and stimulate angiogenesis [12–15]. However, BBGs quickly release alkaline ions, creating a basic pH environment [5,16]. This increase in pH is toxic to cells under static conditions in vitro [12,17]. Blood and most of the interstitial fluids in the human body have an average pH level of 7.35–7.45, which is considered the physiological pH-neutral range [18]. A recent study demonstrated that preconditioning BGs with cell culture medium will prevent the cytotoxic effects associated with the pH shock induced by the dissolution of an alkaline BG [19]. However, it is still unclear how different pretreating periods and glass concentrations affect cell viability and functions. Furthermore, prolonged preconditioning times are not ideal in clinical or laboratory settings.

Another way to control the local pH of BG is to add phosphate to the glass composition [5,6,20]. Phosphate-based bioactive glasses (PBGs) have generated interest because degradation rates can be controlled, ion release can be customized, and the glass can influence the local pH [21–24]. A previous study showed that adding phosphate to a calcium-silicate can counteract the release of alkaline ions and reduce the local pH without pretreating the glass before use [25]. A similar effect has been noted for the addition of phosphate to an alkaline BBG [26]. The dissolution of this borophosphate bioactive glass (BPBG) had little effect on the pH of simulated body fluid. Previously, we evaluated the effects of these BPBGs on endothelial cells in vitro and in vivo. We found that pH-neutral glasses supported endothelial cell migration and stimulated greater blood vessel formation than either the basic BBG or acidic PBG [27]. The current study evaluates the effects of three of those glasses on adipose stem cells (ASCs).

ASCs are isolated from the stromal vascular fraction of subcutaneous fat. This makes them more accessible than their bone marrow counterpart, bone-marrow-derived mesenchymal stem cells (BMSCs). This less invasive harvest allows cells to be collected from any patient, even patients with advanced age or chronic health disorders, and typically provides a more significant number of cells than the harvest of BMSCs [28–30]. Additionally, ASCs have a higher proliferative capacity than BMSCs, reducing the time and need for in vitro expansion. Overall, ASCs have a comparable therapeutic effect to the more studied BMSCs and have been shown to have immunomodulatory properties, angiogenic abilities, and differentiation capacity [30–32]. It is believed that the therapeutic effect of ASCs primarily results from their secretome, which are proteins secreted into the extracellular space [33–36]. The secretome has an essential role for ASCs as a therapeutic cell, including maintaining homeostasis, tissue and organ development, cell signaling, and organizing extracellular matrix [37]. Compared to BMSCs, the secretome of ASCs is more angiogenic and neuro-regenerative [37]. There is increased interest in isolating the secretome from therapeutic cells because of the advantages of that over cell therapy, including scalability, potential reproducibility, availability, and longer shelf lives. The secretome is often overlooked when evaluating biomaterials. However, as this is a fundamental mechanism in tissue regeneration, this study evaluates this novel BPBG series on the ASC secretome.

2. Materials and Methods

2.1. Materials

Table 1 presents a list of reagents and materials utilized in this study.

Table 1. Reagents used in this study.

Reagent	Vendor	Location
α-MEM	Sigma	St Louis, MO, USA
Adipogenic Media	Lonza	Walkersville, MD, USA
Alizarin Red	Sigma	St Louis, MO, USA
Antibiotic/antimycotic	Sigma	St Louis, MO, USA
ASCs	Obatala Sciences, LLC	New Orleans, LA, USA
$CaCO_3$	Fisher Scientific	Rochester, NY, USA
$Ca(PO_3)_2$	Shanghai Muhong Industrial Co, Ltd.	Shanghai, China
Endothelial Cell Media	Lonza	Walkersville, MD, USA
FBS	VWR	Dixon, IL, USA
H_3BO_3	Fisher Scientific	Rochester, NY, USA
H_3PO_4	Fisher Scientific	Rochester, NY, USA
HMVEC-d	Lonza	Walkersville, MD, USA
L-glutamine	Sigma	St Louis, MO, USA

Table 1. *Cont.*

Reagent	Vendor	Location
Live/Dead stain	Fisher Scientific	Rochester, NY, USA
Na_2CO_3	Alfa Aesar	Ward Hill, MA, USA
$NaPO_3$	Shanghai Muhong Industrial Co, Ltd.	Shanghai, China
Oil Red O	Sigma	St Louis, MO, USA
Osteogenesis Media	Lonza	Walkersville, MD, USA
PBS	Sigma	St Louis, MO, USA
Quantibody Array	RayBiotech	Norcross, GA, USA
Trypsin/EDTA	Sigma	St Louis, MO, USA

2.2. Glass Preparation

Preparation of the glasses used in this study are described in Freudenberger et al. [38]. Briefly, glasses with the nominal molar compositions $16Na_2O$-$24CaO$-xB_2O_3-$(60-x)P_2O_5$ were prepared and designated by their respective borate contents, as shown in Table 2. Induction coupled plasma-optical emission spectroscopy (ICP-OES) on an Avio 200 spectrometer (PerkinElmer; Waltham, MA, USA) was used to characterize glass composition. These values were previously reported in Freudenberger et al. [38]. Reagent-grade batch materials were calcined at 300 °C for at least 4 h and, then, melted in platinum crucibles from 1000 to 1150 °C, depending on composition. Melts were stirred with a platinum stir rod on the half hour during melting and, then, quenched in graphite molds after one hour. Samples were annealed at 350 °C for one hour and, then, cooled to room temperature. Glasses were confirmed to be fully amorphous by X-ray diffraction (XRD), using a PANalytical X'Pert Multipurpose diffractometer utilizing a Cu K-a source and a PIXcel Detector. Glasses were ground into 75–150 μm particles and stored in a vacuum desiccator until use.

Table 2. Compositions of the BPBGs used in this study (mol %) as determined by ICP-OES analysis and their respective melt temperatures (T_m). Compositions collected in triplicate and standard deviation reported [38].

Glass Designation	Na_2O	CaO	B_2O_3	P_2O_5	T_m (°C)
X0	14.2 ± 0.1	25.5 ± 0.1	0.0 ± 0.3	60.4 ± 0.5	1050
X40	14.1 ± 0.1	24.2 ± 0.2	40.6 ± 0.2	21.2 ± 0.1	1150
X60	15.2 ± 0.1	24.3 ± 0.2	60.5 ± 0.2	0.0 ± 0.0	1000

2.3. Cell Culture

2.3.1. Adipose Stem Cells

ASCs were prepared by thawing frozen vials of approximately 1×10^6 cells (Obatala Sciences, LLC, New Orleans, LA, USA) into 150 cm² culture plates (Nunc, Rochester, NY, USA) in 20 mL complete culture media (CCM) consisting of alpha minimum essential media (α-MEM; Sigma; St. Louis, MO, USA), 10% fetal bovine serum (FBS; VWR, Dixon, CA, USA), 1% 100x L-glutamine (Sigma, St Louis, MO, USA), and 1% 100× antibiotic/antimycotic (Sigma). After 24 h of incubation at 37 °C humidified and 5% CO_2, media was removed, and the adherent, viable cells were washed twice with phosphate-buffered solution (PBS; Sigma) and harvested using 0.25% trypsin/1 mM Ethylenediamine-tetraacetic acid (EDTA; Sigma, St Louis, MO, USA). ASCs were then plated at 100 cells/cm² in CCM. The media was changed every 3–4 days, and subconfluent cells (≤70% confluent) from three separate donors between passages 2 and 6 were used for all experiments. Donors were Caucasian females aged 28, 34, and 34 with BMIs of 25.65, 22.03, and 20.34, respectively.

2.3.2. Dermal Microvascular Endothelial Cells

Human dermal microvascular endothelial cells (HMVEC-d, pooled donors) were obtained from Lonza (Walkersville, MA, USA). HMVECs were grown under standard conditions in Endothelial Cell Basal Medium-2 (Lonza; Walkersville, MA, USA), and media was changed every 3–4 days.

2.4. Glass Characterization

Approximately 2.5 mg/mL of X0, X40, or X60 glass particles was dissolved in CCM, added to cell culture, and incubated under normal static conditions for 5 or 24 h. Media was then collected, and the room temperature pH of each glass-doped culture was measured. Afterwards, the media was diluted with 1% HNO_3 to obtain solutions with ion concentrations in the 1–20 ppm range. The concentration of ions released from the glasses was measured using inductively coupled plasma-optical emission spectroscopy (ICP-OES) on an Avio 200 spectrometer (PerkinElmer; Waltham, MA, USA). Glass-free CCM was used as a control. Samples were run in triplicate, and averages are reported.

2.5. Cell Viability

ASCs were plated in 8-chambered slides (LabTek; ThermoFisher; Rochester, NY) and grown to 70% confluence under normal static conditions. Approximately 2.5 mg/mL of X0, X40, or X60 glass dissolved in CCM was added to the cells for 24 or 72 h. After incubation at 37 °C humidified with 5% CO_2, chambers were gently washed 3–4 times in pre-warmed PBS and stained with live/dead stain (Fisher Scientific, Pittsburg, PA, USA). Micrographs were taken with a $10\times$ objective on a Nikon A1R-HD/Ti2 E inverted confocal microscope (Melville, NY, USA) and quantified by Fiji software, version 2.7.0 (Madison, Wisconsin).

2.6. Differentiation

ASCs were cultured in 6-well plates at 37 °C, 5% CO_2 until 100% confluent in CCM. A solution of 2.5 mg/mL X0, X40, or X60 glass dissolved in CCM was added to the wells and incubated for 24 h under static conditions. Media was aspirated; wells were gently washed twice with PBS, and differentiation media was added. Adipogenic induction media (Lonza; Walkersville, MD) consisted of 1 mM Dexamethasone, 0.5 mM methyl-isobutyl xanthine, 10 mg/mL insulin, 100 mM indomethacin, and 10% FBS in DMEM (4.5 g/L glucose). Osteogenic induction media (Lonza) consisted of 50 mM ascorbate-2-phosphate, 10 mM b-glycerolphosphate, and 10^{28}M dexamethasone. Media was changed every 3–4 days for 14 days. Cells were washed gently with PBS and fixed in 10% formalin for 1 h at room temperature. Cells were stained with 0.5% Oil Red O to visualize fat droplets or with 40 mM Alizarin Red (pH 4.1) to measure calcium deposition. Differentiation was imaged with an inverted microscope (Leica DMi1; Heerbrugg, Switzerland). Data were quantified using Fiji software, version 2.7.0. (Madison, Wisconsin).

2.7. Migration

Cell migration assays were performed in a 96-well transwell with 8 mm pore membrane inserts (BD Biosciences, Bedford, MA, USA). To evaluate if ASCs were attracted to BPBG, 5.0×10^4 ASCs were suspended in serum-free (SF) media and were added to the top of the transwell inserts. Approximately 2.5 mg/mL X0, X40, or X60 glass was suspended in CCM and added to the bottom of the transwells. After 5 h of incubation at 37 °C, 5% CO_2, the transwell insert was removed and gently placed into trypsin/EDTA. Cells that had migrated to the bottom of the insert were stained with CyQuant and quantified using a fluorescent microplate reader (Fluostar Omega; BMG Labtech, Cary, NC, USA).

To evaluate if BPBG could increase the angiogenic ability of ASCs, the cells were treated with 2.5 mg/mL of X0, X40, or X60 glass in CCM for 24 h. Media was then collected, filtered to remove any remaining glass, and placed in the lower chamber of a transwell. Around 2×10^4 HMVEC-d were added to the top of the inserts and incubated for 5 h.

HMVEC-d that migrated to the bottom of the inserts were stained with CyQuant and read on a plate reader. Each experiment was performed in triplicate.

2.8. Cytokine Array

Subconfluent ASCs were incubated with 2.5 mg/mL of X0, X40, X60, or CCM. After 24 h of incubation, 200 μL of conditioned media was collected, filtered to remove any remaining glass, and analyzed using the Human Cytokine Quantibody Array 4000 (RayBiotech, Norcross, GA, USA) following the manufacturer's instructions. Based on the concentration hierarchy, cytokine concentration data were sorted on Microsoft Excel spreadsheets. A log base 2 of the ratio of the significant protein concentration datasets compared to the control was calculated and used in designing the hierarchal clustered heatmaps. These experiments were performed in duplicates on pooled conditioned media from three ASC donors.

2.9. Statistics

Each experiment was performed in triplicate with a minimum of three separate ASC donors. All values are presented as means ± standard deviation (SD). The statistical differences among two or more groups were determined by ANOVA, followed by post hoc Tukey versus the control groups. All statistical analyses were performed using Minitab® Statistical Software (State College, PA, USA).

3. Results

3.1. Glass Properties

Table 3 displays the pH as reported by Freudenberger et al. [39], recorded 24 h post the addition of 3 mg/mL of the three glasses from the current study into DI water at 37ºC. The borate-free X0 glass yielded an acidic solution (pH ~ 2.6); the phosphate free X60 glass produced an alkaline solution (pH ~ 8.5), and the X40 borophosphate glass produced a pH-neutral solution (pH ~ 7). These same glass particles were introduced to ASCs under standard culture conditions, and both the pH and the released ions were measured (Table 3). After 24 h, the pH values of the CCM with the acidic X0 glass and with the pH-neutral X40 glass particles showed no significant differences from the baseline CCM values. However, the CCM pH with the alkaline X60 glass particles exhibited a slight increase. The difference in the pH values from the water experiments and the CCM experiments reflects the buffering effects of the latter.

Table 3. The pH and ion concentration of the cell culture media were measured after interactions with 2.5 mg/mL BPBGs for the specified durations. The pH values for deionized water (DI) correspond to 3 mg/mL of each glass after 24 h, as reported previously [39]. The percent refers to the proportions of ions released from each glass into the media. ND: not detected.
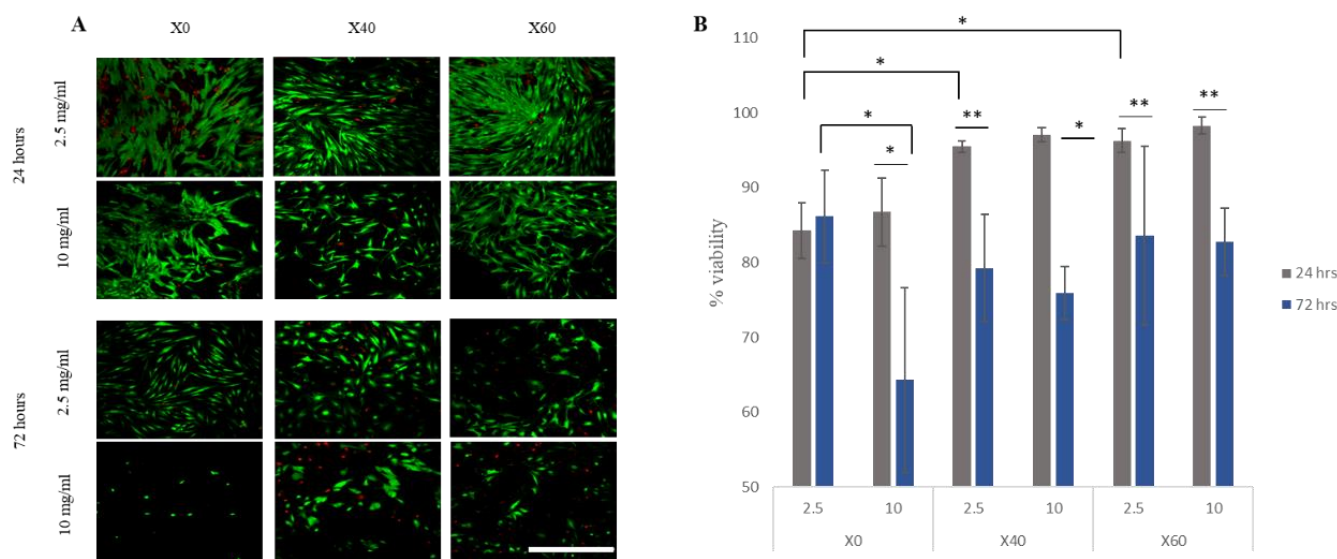
| Sample | Time (h) | pH | | Ions Released | | | | | |
| | | DI | CCM | P | | B | | Ca | |
				ppm	%	ppm	%	ppm	%
CCM	5	ND	7.32	34.80 ± 1.45	ND	ND	ND	65.82 ± 2.68	ND
	24	ND	7.53	36.65 ± 0.88	ND	ND	ND	68.41 ± 1.07	ND
X0	5	ND	7.23	72.04 ± 0.47	4	ND	ND	68.84 ± 2.67	1
	24	2.6	7.49	197.03 ± 5.91	19	ND	ND	101.28 ± 1.64	15
X40	5	ND	7.25	121.06 ± 3.61	22	126.10 ± 1.46	46	82.36 ± 1.37	5
	24	7.1	7.39	176.01 ± 4.24	36	217.40 ± 1.06	80	73.26 ± 1.11	2
X60	5	ND	7.86	23.27 ± 0.30	ND	249.43 ± 8.00	50	173.16 ± 3.79	29
	24	8.6	7.67	24.96 ± 0.18	ND	301.26 ± 6.03	61	201.43 ± 5.03	36

Table 3 also shows the respective concentrations of calcium, borate, and phosphate species in the CCM solutions after 5 h and 24 h with the glass particles. Borate ions were not detected in either the CCM baseline or the CCM after reacting with the X0 particles. However, significant concentrations of borate ions were found in the CCM solutions containing X40 and X60 particles. Approximately 80% of the borate ions were released from the X40 glass, while ~61% of borate ions were released from the X60 glass after 24 h (Table 3). Similar calculations were performed for the phosphate and calcium concentrations in solution, after normalizing for their respective concentrations in the baseline CCM. These values, however, are likely affected by the precipitation of calcium phosphate phases on the surfaces of the reacting glass particles [39]. The calcium ion concentrations of the CCM after 24 h with X0 and X40 glasses were slightly greater than the baseline concentrations, but the CCM with X60 particles had much greater concentrations of calcium ions. For both X0 and X40 glasses, the phosphate content of the CCM solutions increased over the baseline values at both timepoints evaluated. For X60, the phosphate content of the CCM solution decreased from about 36 ppm to 24 ppm after reacting with the X60 glass particles.

The reaction between calcium ions released from the X60 glass and phosphate anions in the CCM to precipitate a calcium phosphate phase likely accounts for the reduction in the phosphate anion concentration in the X60 CCM samples below the baseline values.

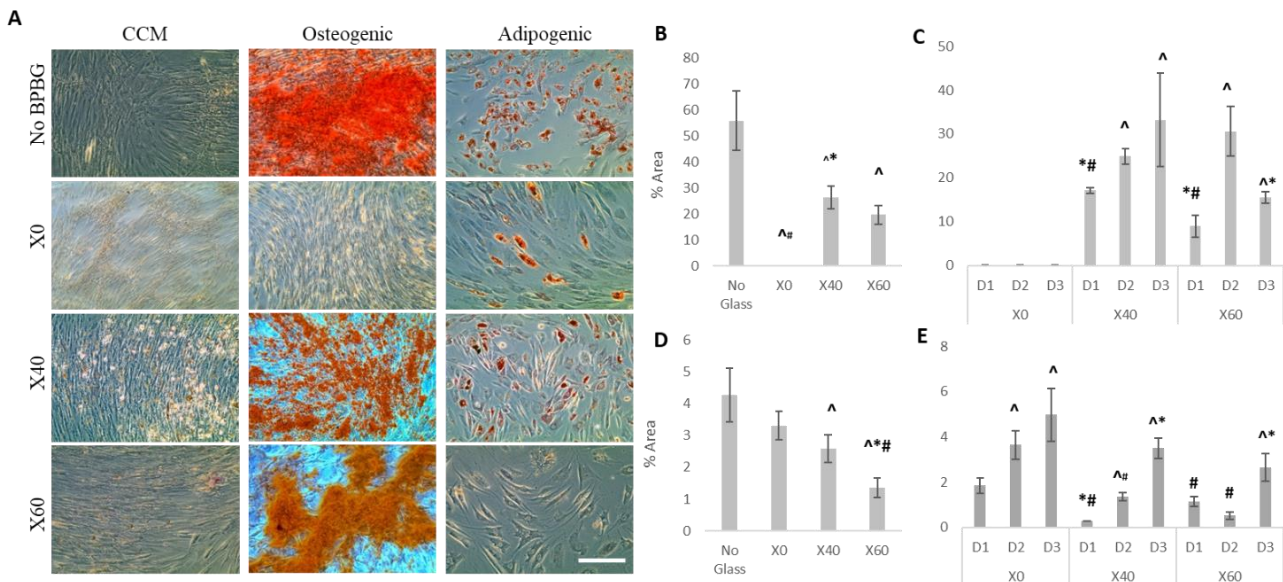### 3.2. A High Concentration of BPBGs Reduced ASC Viability at 72 h

According to the ISO norm, a decrease in cell viability by 30% indicates a biomaterial is toxic and not biocompatible [40]. To evaluate the cytotoxicity effect of BPBGs on ASCs, low and high concentrations (2.5 and 10 mg/mL, respectively) of three glass compositions were directly added to ASCs under normal static conditions (Figure 1). At 24 h, cells remained viable in the presence of all three glass compositions at both low and high concentrations. The acidic X0 glass had the lowest viability at both concentrations, and the only non-viable condition was the high concentration of X0 after 72 h. Interestingly, a low concentration of the same glass maintained its viability, while all other glass compositions and concentrations decreased at that time point.

Figure 1. A high concentration of BPBGs reduced ASC viability at 72 h under static conditions. Subconfluent ASCs were treated with low (2.5 mg/mL) or high (10 mg/mL) concentrations of BPBG. (**A**) Live/dead stain showed ASC viability at 24 and 72 h. Scale bar = 500 μm. (**B**) Viability was quantified with three donors examined in triplicate. Error bars indicate SD (n = 9); * $p \leq 0.01$, and ** $p < 0.5$.
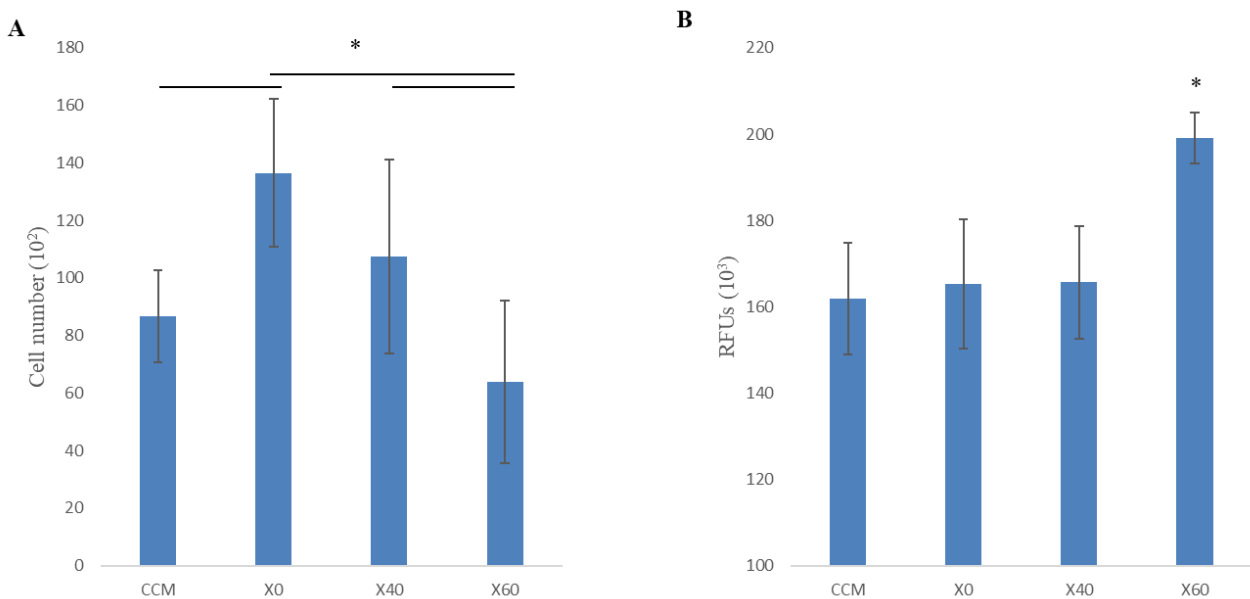
3.3. BPBG Affects ASCs Differentiation

In low-concentration BPBGs, ASCs were tested for their differentiation ability into adipogenic and osteogenic lineages. ASCs were grown to 100% confluency, incubated with X0, X40, or X60 glasses under normal, static conditions for 24 h, and then expanded for 14 days in adipogenic or osteogenic media. The alkaline X60 glass reduced adipogenic differentiation, whereas the acidic X0 glass inhibited osteogenic differentiation (Figure 2). Furthermore, X0 inhibited osteogenesis in all three donors tested, whereas there was a donor variation with all other differentiation assays.

Figure 2. BPBGs influence ASC differentiation. ASCs were induced to differentiate into bone or fat in the absence or presence of BPBG. (**A**) Representative micrographs of 3 ASC donors are shown. Scale bar = 250 μm. Osteogenic (**B**,**C**) and adipogenic (**D**,**E**) differentiation were quantified using Fiji software. Mean ± SD; ˆ $p < 0.05$ compared to no glass control; * $p < 0.05$ compared to X0; # $p < 0.05$ compared to X40. When stimulated with glass, ASC donors showed a difference in osteogenesis (**C**) and adipogenesis (**E**). Mean ± SD; ˆ $p < 0.05$ compared to D1; * $p < 0.05$ compared to D2; # $p < 0.05$ compared to D3.

3.4. pH-Neutral BPBGs Attract ASCs, While ASCs Treated with Alkaline BPBGs Attract ECs

Adipose stem cells possess an inherent ability to migrate to sites of injuries and secrete various chemokines, cytokines, and growth factors that enable them to mediate the regeneration process [41–44]. To test whether different compositions of BPBGs affected the migration of ASCs, a 5 h transwell migration assay was used. Glasses X0 and X40 increased ASC migration, whereas X60 had no statistical effect (Figure 3A).
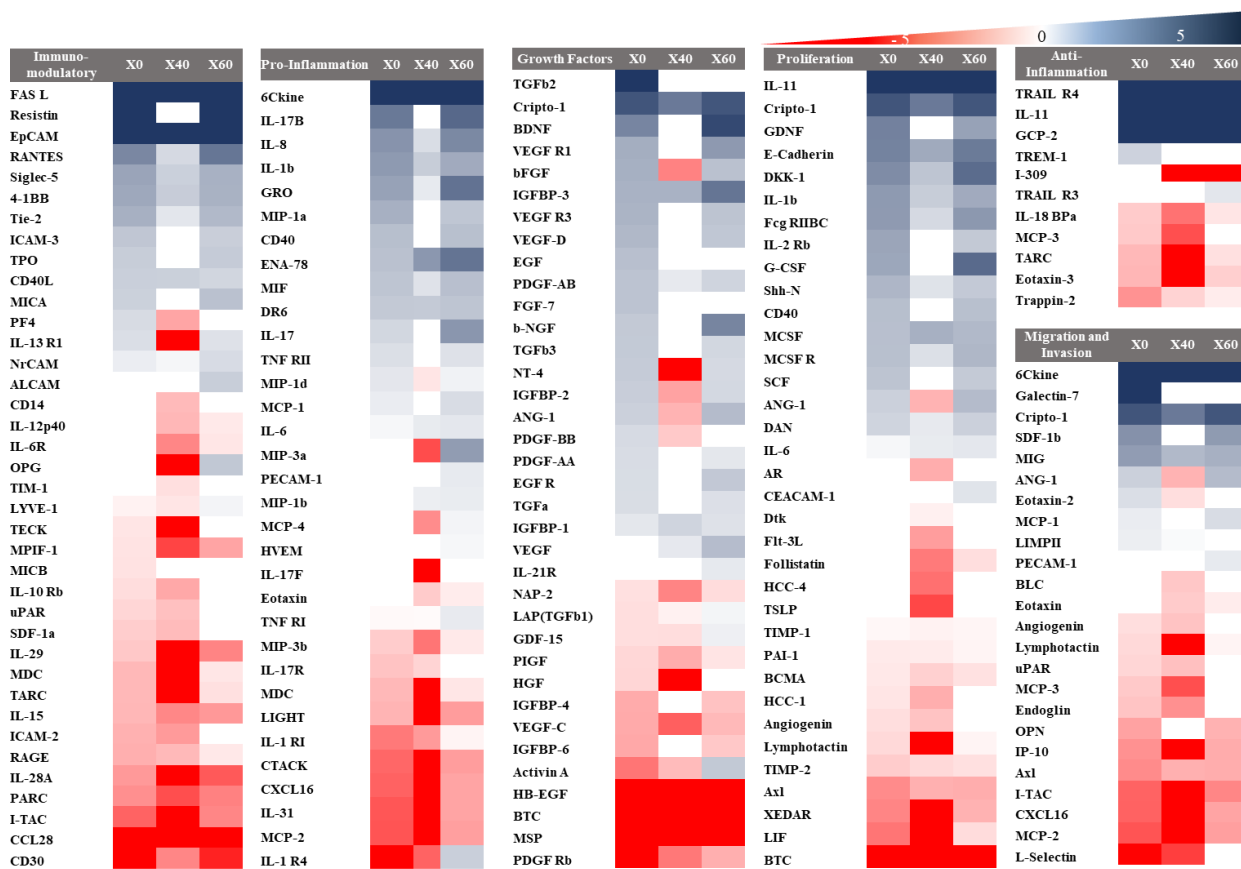
Figure 3. BPBGs affect cell migration. (**A**) A transwell assay examined migration. ASCs were loaded onto the top inserts, while 2.5 mg/mL of glass was added to the bottom. After 5 h of incubation, migrated cells were measured by CyQuant. (**B**) ASCs were treated with glass for 24 h under standard conditions. The resulting conditioned media was put in the bottom of a transwell with ECs added to the top. After 5 h of incubation, migrated cells were measured by CyQuant. In both assays, three separate ASC donors were examined in triplicate. Error bars indicated SD (n = 9); * *p*-value $\leq$ 0.05.
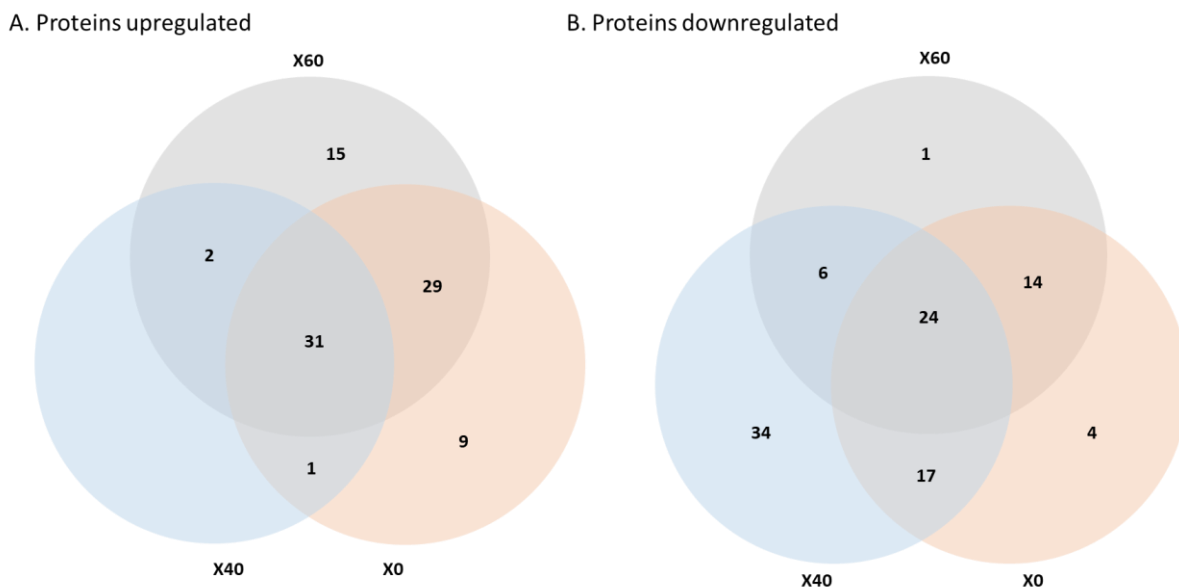
ASCs are also angiogenic, partially due to their ability to attract endothelial cells (ECs) [36]. To test if BPBG could affect the ability of ASCs to attract ECs, subconfluent ASCs were treated with BPBG for 24 h. The resulting conditioned media was used as an attractant for EC migration. Interestingly, only X60 increased the ASCs' ability to attract ECs (Figure 3B).

3.5. BPBG Alters ASC Secretome

A quantitative sandwich-based ELISA array was performed to determine if BPBGs influenced the ASC secretome. After conditioning ASCs with a low concentration of BPBG for 24 h, the conditioned media was examined for 200 secreted proteins, including cytokines, growth factors, proteases, soluble receptors, and others (Figure 4). Of those, 187 proteins were detectable in sufficient expression levels, with glass treatment causing the upregulation of 87 proteins (Figure 5A) and the downregulation of 100 proteins (Figure 5B). Of those that were upregulated, 31 were upregulated with all three glass compositions, with 5 having no detectable levels in untreated ASCs. On the other hand, 24 proteins were downregulated in all three glass compositions, with 4 (BTC, CCL28, MSP, and HB-EGF) completely inhibited in glass treatment. There were 21 proteins that were differentially secreted with boron concentration: 1 decreased, 4 increased from levels detected in CCM, 11 were highest in CCM but then had increasing levels in glass-treated media, and 5 had increasing concentrations with increasing boron but with only X60 being above CCM base levels (Table 4).

Figure 4. Representative hierarchal heatmap clustering the proteins based on function. All proteins presented are significant from the control ($p < 0.5$). Log2(FC) is used in which (-5 to 5) is the range, and any value above 5 is represented as dark blue whereas any value below -5 is represented as dark red color. In contrast, the white color represents all the proteins that are not significant. FC represents the fold change between the samples treated with glass in relation to the control.

Figure 5. Effect of BPBGs on the ASCs secretory profile. Subconfluent ASCs were treated with 2.5 mg/mL of BPBG for 24 h. Media was then collected and analyzed for secreted proteins. ASC protein secretion was increased (**A**) or decreased (**B**) with glass treatment.

Table 4. Protein secretion levels, presented in pg/mL and mean ± SD. Blue color represents the highest expression.

	CCM	X0	X40	X60
I-309	1.77 ± 0.57	1.98 ± 0.00	0.05 ± 0.07	0 ± 0
ENA-78	5.72 ± 0.58	16.91 ± 0.94	34.72 ± 18.34	64.43 ± 19.25
IL-6	2701.45 ± 26.1	3118.31 ± 41.64	3865.87 ± 254.17	4109.95 ± 226.75
MIP-1b	68.36 ± 13.41	70.92 ± 4.68	92.55 ± 2.58	96.42 ± 2.91
VEGF	92.27 ± 2.51	94.50 ± 3.18	137.6 ± 14.54	294.71 ± 7.60
Activin A	280.68 ± 3.43	43.34 ± 4.66	112.34 ± 40.94	725.43 ± 86.71
IL-1R4	68.35 ± 53.92	2.01 ± 2.84	8.3 ± 11.74	158.44 ± 43.02
TGFβ1	32.84 ± 3.69	21.13 ± 1.78	27.32 ± 2.82	39.70 ± 1.17
TNFR1	201.07 ± 8.25	185.55 ± 14.8	188.68 ± 14.05	289.75 ± 0.51
TRAIL R3	22.90 ± 7.87	19.34 ± 1.15	22.52 ± 2.56	35.79 ± 0.92
Contactin-2	54.06 ± 25.45	34.79 ± 23.03	39.99 ± 15.39	41.34 ± 11.09
Dtk	45.79 ± 10.57	29.92 ± 40.39	37.39 ± 6.93	43.84 ± 12.14
IL-1RI	9.29 ± 0.58	1.51 ± 0.18	2.36 ± 0.29	8 ± 1.02
IL-17R	32.17 ± 0.49	14.40 ± 18.02	17.93 ± 1.26	30.14 ± 5.68
L-selectin	149.13 ± 58.12	4.84 ± 6.85	10.85 ± 12.99	144.18 ± 23.18
MICB	356.25 ± 61.86	241.29 ± 140.6	322.14 ± 82.21	339.68 ± 24.5
PAI-1	4466.23 ± 255.95	3381.66 ± 472.87	3408.96 ± 451.51	3876.75 ± 261.23
PDGF Rb	441.62 ± 174.57	0 ± 0	70.73 ± 99.85	149.87 ± 193.95
RAGE	7.73 ± 1.51	2.63 ± 2.2	3.02 ± 2.71	5.72 ± 1.28
TIMP-2	12,795.45 ± 1190.17	6473.49 ± 1026.09	7645.48 ± 155.76	8481.24 ± 400.92
Trappin-2	15.2 ± 1.92	3.47 ± 0.47	8.47 ± 2.55	11.78 ± 0.54

4. Discussion

Because alkaline glasses can be toxic to cells and tissues, they are often pre-reacted before use in cell culture. Even BPBGs have been pre-reacted to evaluate ion release on ASC viability [45]. This makes cell culture and potential clinical applications of BGs complicated. To understand the role of BGs in the clinic, evaluating them in direct contact with cells is essential. Furthermore, it is also necessary to understand if the effects of BGs are due to the change in pH or due to different ion release rates. For example, the CCM samples with X0 and X40 particles had similar values of pH after 5 h of incubation with ASCs, but the phosphate content of the CCM with the X40 particles was about 68% larger than the phosphate content of the CCM with the X0 particles. In addition, the X40 particles released a significant concentration (126 ppm) of borate species to the CCM. Therefore, differences in cell phenotype and function between X0 and X40 treatment are probably attributable to ion release rather than solely to the change in pH levels of the entire media.

At 2.5 mg/mL, the phosphate-rich acidic X0 glass maintained cell viability over 72 h, better than the glasses with lower phosphate contents. However, at 10 mg/mL, X0 glass was considered non-viable at the same time point. This correlates with other studies showing that increasing extracellular inorganic phosphate levels promotes cell growth and proliferation, while increasing the concentration (above 16mM) triggers cell death by activating both intrinsic and extrinsic apoptotic pathways [46].

Our results show that ASCs act as buffers, making the extracellular environment more pH-neutral when in the presence of BGs. Though little is known about the ability of ASCs to regulate extracellular pH, it is understood that cells can maintain a narrow range (7.1–7.2) of intracellular pH through the actions of membrane proton pumps and transporters, which are controlled by intra-cytoplasmic pH sensors [47]. These sensors can recognize and induce cellular responses to maintain the intracellular pH, often at the expense of acidifying the extracellular pH. In turn, extracellular acidification impacts G-protein-coupled receptors (GPCRs). There is evidence that the expression of proton-sensing GPCRs can regulate the migration and invasion of cells, which may explain why acidic X0 increased ASC migration the most. On the other hand, elevated levels of extracellular inorganic phosphate have been

shown to induce epithelial-mesenchymal transition through ERK1/2 signaling, promoting cell migration and invasiveness during development, cancer metastasis, wound healing, and fibrosis [46]. The exact mechanism for the increased migration, extracellular pH, or increased extracellular phosphate needs to be explored to consider the use of the X0 glass.

BMSCs, with similar properties to ASCs, are known to migrate during the initial stages of wound healing. During this inflammatory phase, the pH of the damaged area decreases to an acidic condition [47]. In our study, ASCs demonstrated increased migration to X0 as it degraded over 5 h. Because X0 and X40 had similar pH effects on the cell culture media at this time point, this suggests that the migration difference is due to the ions present and not solely the pH. Consequently, it is worth noting that X0 released the lowest amount of calcium ions at this time point. Calcium has long been known to be a crucial regulator and mediator in cell migration [48–50]. Previous research on BMSCs showed that calcium has an optimal compositional range to promote BMSC migration [51]. The X40 and X60 glasses may release too much calcium to effectively stimulate downstream genes of GPCR signaling pathways, an early response to calcium-based biomaterials [48]. Consequently, the calcium-sensing receptor (CaSR), a receptor belonging to the GPCR family that modulates the chemotactic response of MSCs in response to extracellular calcium, may be stimulated by the X0 glass and not the X40 or X60 glasses.

In our study, we showed that after 24 h, only the boron-rich X60 glass increased the angiogenic ability of ASCs by attracting endothelial cells, as well as increased secreted angiogenic molecules, such as VEGF, ANG-1, b-NGF, IGFBP-3, TGFb3, and bFGF. This agrees with other studies that have shown the impact of borate released from BBGs on angiogenesis [14,49–52].

The phosphate-rich, acidic X0 glass completely inhibited osteogenesis in all three ASC donors. The adipogenic ability was also reduced compared to the controls, though not significantly. This correlates with the observation that pre-treating MSCs with an acidic environment enhances the stemness of MSCs, thus resulting in a lack of differentiation ability [53]. The borate-rich, alkaline X60 glass, on the other hand, reduced adipogenic differentiation. This coincides with previous work showing that boron prevented lipid deposition and suppressed adipogenesis transcriptional programming while maintaining cell viability [54]. Interestingly, despite all donors being similar in age, BMI, race, and sex, there was a donor difference in all differentiation assays except for X0 treatment in osteogenesis. The differences in donors' phenotypic changes from glass treatment warrant further investigation.

Most of the literature on bioactive glass, including BPBG, focuses on cell viability, proliferation, or differentiation of ASCs [45,55–57]. However, there is very little reported on the effect of BG on the ASC secretome. ASCs have a broad secretory profile of different growth factors, cytokines, and other proteins that impact the body's response to injuries, healing, and tissue regeneration. These secreted proteins all work to keep the body in homeostasis [33,58]. The present study showed that BPBGs can alter the ASC's secretome.

Our study showed that, regardless of the glass composition, the expression of 6-Ckine, EpCAM, FasL, TRAIL R4, and IL-4 was promoted, while they were not secreted without any of the glass treatments. Each of these biomolecules is worth investigating, as BGs may be used as a cell treatment to increase the efficacy of the cells. For example, IL-4 overexpression in BMSCs polarized macrophages from an inflammatory M1 macrophage into a tissue regenerative M2 phenotype [59]. Evaluating these molecules will allow biomaterial designers to cater their materials for different applications.

ASCs treated with the pH-neutral X40 glass increased the secretion of anti-proliferation and anti-migration proteins. Because X40 and X0 had similar effects on the pH of the extracellular fluid, the pH cannot be solely responsible for the increase in these proteins. The greater borate or phosphate release from X40 may have impacted the function of ASCs. The concentration of borate ions affected the ability of ASCs to secrete 22 proteins: 2 decreased with increased borate while 20 increased, which included many pro-inflammatory (IL-1, IL-6, IL17, etc.) and angiogenic (VEGF, L-Selectin, TIMP-2, etc) proteins. As borate is

anti-inflammatory in other applications, it is worth looking into how the controlled release of borate ions in different pH ranges may have different control over cells [60]. These results correlate to previous work from other groups showing that the release of therapeutic ions from bioactive glass influences cell function and phenotype [6,12,61].

One limitation of this study is that the pH was measured from the extracellular fluid in its entirety and not at the cell surface. Although the ions released from the glass most likely impacted cell phenotype, it is uncertain if the ions contributed to a localized change in pH near the cell surface. Bioactive glasses have the ability to alter local pH [21–24]. Cells use pH gradients, local heterogeneity, and dynamic fluctuations to regulate biophysical phenomena, such as metabolism, migration, vesicular traffic, and the spatial organization of tissues during development [62]. The fluctuation of the pH gradient at the cell surface can determine cell fate by activating molecular pathways, for example via the GPCR, a family of proton-sensing receptors on cell membranes [63]. An instance of this phenomenon is observed in the acidity of the environment surrounding cancer cells, which tends to decrease as the distance from the cell membrane increases [64,65]. Though less is known about the impact of localized pH at the surface of ASCs, or even BMSCs, studies on cancer and immune cells show that certain GPCRs influence cell reprogramming and differentiation [63].

5. Conclusions

The development of bioactive glasses holds promise for a variety of applications in regenerative medicine, tissue engineering, drug delivery, and beyond. Bioactive glasses have already shown potential in the clinic for bone regeneration, wound healing, and dental applications due to their ability to stimulate tissue growth and integrate with surrounding tissues. One area of interest is developing bioactive glasses that can create or maintain pH-neutral environments. In addition to the clinical benefits of a pH-neutral biomaterial, this will allow the glasses to be in direct contact with cells in culture, increasing their use in 3D bioprinting, scaffold fabrication, and the creation of complex structures that mimic the properties of natural tissues, enhancing their integration and functionality in vivo. A pH-neutral bioactive glass will negate the often necessary pre-reaction required for alkaline and acidic glasses, making both cell culture and potential clinical use of bioactive glasses intricate.

Overall, our study sheds light on the impact of bioactive glasses on ASCs' secretome, revealing alterations in the expression of several biomolecules. These findings have implications for designing biomaterials tailored to specific applications, as ASCs are found in several locations throughout the body. However, it is important to note limitations, such as the need to explore localized pH effects at the cell surface and further investigate how ion release influences cell function. As our understanding of bioactive glass interactions with cells and tissues advances, we can anticipate refinements in their formulation and design tailored glasses to specific clinical needs. This will allow their use for a wide range of medical conditions, including cardiovascular diseases, neurological disorders, and even cancer.

Institutional Review Board Statement: Not applicable.

Data Availability Statement: The datasets generated during the current study are available from the corresponding author with reasonable request.

Conflicts of Interest: The authors declare no conflicts of interest.

References

1. Hench, L.L. The story of Bioglass®. *J. Mater. Sci. Mater. Med.* **2006**, *17*, 967–978. [CrossRef] [PubMed]
2. Baino, F.; Hamzehlou, S.; Kargozar, S. Bioactive Glasses: Where Are We and Where Are We Going? *J. Funct. Biomater.* **2018**, *9*, 25. [CrossRef] [PubMed]
3. Kaur, G.; Pandey, O.P.; Singh, K.; Homa, D.; Scott, B.; Pickrell, G. A review of bioactive glasses: Their structure, properties, fabrication and apatite formation. *J. Biomed. Mater. Res. Part A* **2014**, *102*, 254–274. [CrossRef]
4. Rahaman, M.N.; Day, D.E.; Bal, B.S.; Fu, Q.; Jung, S.B.; Bonewald, L.F.; Tomsia, A.P. Bioactive glass in tissue engineering. *Acta Biomater.* **2011**, *7*, 2355–2373. [CrossRef] [PubMed]
5. Hoppe, A.; Güldal, N.S.; Boccaccini, A.R. A review of the biological response to ionic dissolution products from bioactive glasses and glass-ceramics. *Biomaterials* **2011**, *32*, 2757–2774. [CrossRef]
6. Mehrabi, T.; Mesgar, A.S.; Mohammadi, Z. Bioactive Glasses: A Promising Therapeutic Ion Release Strategy for Enhancing Wound Healing. *ACS Biomater. Sci. Eng.* **2020**, *6*, 5399–5430. [CrossRef]
7. Yao, A.; Wang, D.; Huang, W.; Fu, Q.; Rahaman, M.N.; Day, D.E. In Vitro Bioactive Characteristics of Borate-Based Glasses with Controllable Degradation Behavior. *J. Am. Ceram. Soc.* **2007**, *90*, 303–306. [CrossRef]
8. Fu, Q.; Rahaman, M.N.; Fu, H.; Liu, X. Silicate, borosilicate, and borate bioactive glass scaffolds with controllable degradation rate for bone tissue engineering applications. I. Preparation and in vitro degradation. *J. Biomed. Mater. Res. Part A* **2010**, *95*, 164–171. [CrossRef]
9. Huang, W.; Day, D.E.; Kittiratanapiboon, K.; Rahaman, M.N. Kinetics and mechanisms of the conversion of silicate (45S5), borate, and borosilicate glasses to hydroxyapatite in dilute phosphate solutions. *J. Mater. Sci. Mater. Med.* **2006**, *17*, 583–596. [CrossRef]
10. Fu, H.; Fu, Q.; Zhou, N.; Huang, W.; Rahaman, M.N.; Wang, D.; Liu, X. In vitro evaluation of borate-based bioactive glass scaffolds prepared by a polymer foam replication method. *Mater. Sci. Eng. C* **2009**, *29*, 2275–2281. [CrossRef]
11. Zhang, J.; Guan, J.; Zhang, C.; Wang, H.; Huang, W.; Guo, S.; Niu, X.; Xie, Z.; Wang, Y. Bioactive borate glass promotes the repair of radius segmental bone defects by enhancing the osteogenic differentiation of BMSCs. *Biomed. Mater. Bristol Engl.* **2015**, *10*, 065011. [CrossRef]
12. Kargozar, S.; Baino, F.; Hamzehlou, S.; Hill, R.G.; Mozafari, M. Bioactive Glasses: Sprouting Angiogenesis in Tissue Engineering. *Trends Biotechnol.* **2018**, *36*, 430–444. [CrossRef]
13. Zhao, S.; Li, L.; Wang, H.; Zhang, Y.; Cheng, X.; Zhou, N.; Rahaman, M.N.; Liu, Z.; Huang, W.; Zhang, C. Wound dressings composed of copper-doped borate bioactive glass microfibers stimulate angiogenesis and heal full-thickness skin defects in a rodent model. *Biomaterials* **2015**, *53*, 379–391. [CrossRef]
14. Balasubramanian, P.; Hupa, L.; Jokic, B.; Detsch, R.; Grünewald, A.; Boccaccini, A.R. Angiogenic potential of boron-containing bioactive glasses: In vitro study. *J. Mater. Sci.* **2017**, *52*, 8785–8792. [CrossRef]
15. Thyparambil, N.J.; Gutgesell, L.C.; Hurley, C.C.; Flowers, L.E.; Day, D.E.; Semon, J.A. Adult stem cell response to doped bioactive borate glass. *J. Mater. Sci. Mater. Med.* **2020**, *31*, 13. [CrossRef]
16. Jones, J.R.; Sepulveda, P.; Hench, L.L. Dose-dependent behavior of bioactive glass dissolution. *J. Biomed. Mater. Res.* **2001**, *58*, 720–726. [CrossRef]
17. Qazi, T.H.; Hafeez, S.; Schmidt, J.; Duda, G.N.; Boccaccini, A.R.; Lippens, E. Comparison of the effects of 45S5 and 1393 bioactive glass microparticles on hMSC behavior. *J. Biomed. Mater. Res. Part A* **2017**, *105*, 2772–2782. [CrossRef]
18. Kellum, J.A. Determinants of blood pH in health and disease. *Crit. Care Lond. Engl.* **2000**, *4*, 6–14. [CrossRef]
19. Hohenbild, F.; Arango-Ospina, M.; Moghaddam, A.; Boccaccini, A.R.; Westhauser, F. Preconditioning of Bioactive Glasses before Introduction to Static Cell Culture: What Is Really Necessary? *Methods Protoc.* **2020**, *3*, 38. [CrossRef]
20. Carta, D.; Qiu, D.; Guerry, P.; Ahmed, I.; Neel, E.A.A.; Knowles, J.C.; Smith, M.E.; Newport, R.J. The effect of composition on the structure of sodium borophosphate glasses. *J. Non-Cryst. Solids* **2008**, *354*, 3671–3677. [CrossRef]
21. Ahmed, I.; Lewis, M.; Olsen, I.; Knowles, J.C. Phosphate glasses for tissue engineering: Part 1. Processing and characterisation of a ternary-based P_2O_5–CaO–Na_2O glass system. *Biomaterials* **2004**, *25*, 491–499. [CrossRef]
22. Ahmed, I.; Lewis, M.; Olsen, I.; Knowles, J.C. Phosphate glasses for tissue engineering: Part 2. Processing and characterisation of a ternary-based P_2O_5-CaO-Na_2O glass fibre system. *Biomaterials* **2004**, *25*, 501–507. [CrossRef]
23. Mneimne, M.; Hill, R.G.; Bushby, A.J.; Brauer, D.S. High phosphate content significantly increases apatite formation of fluoride-containing bioactive glasses. *Acta Biomater.* **2011**, *7*, 1827–1834. [CrossRef]
24. Saranti, A.; Koutselas, I.; Karakassides, M.A. Bioactive glasses in the system CaO–B_2O_3–P_2O_5: Preparation, structural study and in vitro evaluation. *J. Non-Cryst. Solids* **2006**, *352*, 390–398. [CrossRef]
25. Li, A.; Lv, Y.; Ren, H.; Cui, Y.; Wang, C.; Martin, R.A.; Qiu, D. In vitro evaluation of a novel pH neutral calcium phosphosilicate bioactive glass that does not require preconditioning prior to use. *Int. J. Appl. Glass Sci.* **2017**, *8*, 403–411. [CrossRef]
26. Massera, J.; Shpotyuk, Y.; Sabatier, F.; Jouan, T.; Boussard-Plédel, C.; Roiland, C.; Bureau, B.; Petit, L.; Boetti, N.G.; Milanese, D.; et al. Processing and characterization of novel borophosphate glasses and fibers for medical applications. *J. Non-Cryst. Solids* **2015**, *425*, 52–60. [CrossRef]
27. Bromet, B.A.; Blackwell, N.P.; Abokefa, N.; Freudenberger, P.; Blatt, R.L.; Brow, R.K.; Semon, J.A. The angiogenic potential of pH-neutral borophosphate bioactive glasses. *J. Biomed. Mater. Res. Part A* **2023**, *111*, 1554–1564. [CrossRef] [PubMed]
28. Dykstra, J.A.; Facile, T.; Patrick, R.J.; Francis, K.R.; Milanovich, S.; Weimer, J.M.; Kota, D.J. Concise Review: Fat and Furious: Harnessing the Full Potential of Adipose-Derived Stromal Vascular Fraction. *Stem Cells Transl. Med.* **2017**, *6*, 1096–1108. [CrossRef]

29. Gimble, J.M.; Guilak, F.; Bunnell, B.A. Clinical and preclinical translation of cell-based therapies using adipose tissue-derived cells. *Stem Cell Res. Ther.* **2010**, *1*, 19. [CrossRef]

30. Bourin, P.; Bunnell, B.A.; Casteilla, L.; Dominici, M.; Katz, A.J.; March, K.L.; Redl, H.; Rubin, J.P.; Yoshimura, K.; Gimble, J.M. Stromal cells from the adipose tissue-derived stromal vascular fraction and culture expanded adipose tissue-derived stromal/stem cells: A joint statement of the International Federation for Adipose Therapeutics and Science (IFATS) and the International Society for Cellular Therapy (ISCT). *Cytotherapy* **2013**, *15*, 641–648. [CrossRef]

31. De Francesco, F.; Ricci, G.; D'Andrea, F.; Nicoletti, G.F.; Ferraro, G.A. Human Adipose Stem Cells: From Bench to Bedside. *Tissue Eng. Part B Rev.* **2015**, *21*, 572–584. [CrossRef] [PubMed]

32. Al-Nbaheen, M.; Vishnubalaji, R.; Ali, D.; Bouslimi, A.; Al-Jassir, F.; Megges, M.; Prigione, A.; Adjaye, J.; Kassem, M.; Aldahmash, A. Human Stromal (Mesenchymal) Stem Cells from Bone Marrow, Adipose Tissue and Skin Exhibit Differences in Molecular Phenotype and Differentiation Potential. *Stem Cell Rev. Rep.* **2013**, *9*, 32–43. [CrossRef] [PubMed]

33. Lombardi, F.; Palumbo, P.; Augello, F.R.; Cifone, M.G.; Cinque, B.; Giuliani, M. Secretome of Adipose Tissue-Derived Stem Cells (ASCs) as a Novel Trend in Chronic Non-Healing Wounds: An Overview of Experimental In Vitro and In Vivo Studies and Methodological Variables. *Int. J. Mol. Sci.* **2019**, *20*, 3721. [CrossRef] [PubMed]

34. Li, X.; Ma, T.; Sun, J.; Shen, M.; Xue, X.; Chen, Y.; Zhang, Z. Harnessing the secretome of adipose-derived stem cells in the treatment of ischemic heart diseases. *Stem Cell Res. Ther.* **2019**, *10*, 196. [CrossRef]

35. Kumar, P.; Kandoi, S.; Misra, R.; Vijayalakshmi, S.; Rajagopal, K.; Verma, R.S. The mesenchymal stem cell secretome: A new paradigm towards cell-free therapeutic mode in regenerative medicine. *Cytokine Growth Factor Rev.* **2019**, *46*, 1–9. [CrossRef] [PubMed]

36. Kilroy, G.E.; Foster, S.J.; Wu, X.; Ruiz, J.; Sherwood, S.; Heifetz, A.; Ludlow, J.W.; Stricker, D.M.; Potiny, S.; Green, P.; et al. Cytokine profile of human adipose-derived stem cells: Expression of angiogenic, hematopoietic, and pro-inflammatory factors. *J. Cell. Physiol.* **2007**, *212*, 702–709. [CrossRef] [PubMed]

37. Gorgani, S.; Hosseini, S.A.; Wang, A.Z.; Baino, F.; Kargozar, S. Effects of Bioactive Glasses (BGs) on Exosome Production and Secretion: A Critical Review. *Mater. Basel Switz.* **2023**, *16*, 4194. [CrossRef] [PubMed]

38. Freudenberger, P.T.; Blatt, R.L.; Youngman, R.E.; Brow, R.K. Network structures and the properties of Na-Ca-Sr-borophosphate glasses. *J. Non-Cryst. Solids* **2023**, *600*, 121966. [CrossRef]

39. Freudenberger, P.T.; Blatt, R.L.; Brow, R.K. Dissolution rates of borophosphate glasses in deionized water and in simulated body fluid. *J. Non-Cryst. Solids X* **2023**, *18*, 100181. [CrossRef]

40. *ISO 10993-5:2009*; Biological Evaluation of Medical Devices Part 5: Tests for In Vitro Cytotoxicity. ISO: Geneva, Switzerland, 2022. Available online: https://www.iso.org/standard/36406.html (accessed on 5 March 2024).

41. Baek, S.J.; Kang, S.K.; Ra, J.C. In vitro migration capacity of human adipose tissue-derived mesenchymal stem cells reflects their expression of receptors for chemokines and growth factors. *Exp. Mol. Med.* **2011**, *43*, 596–603. [CrossRef]

42. de Lucas, B.; Pérez, L.M.; Gálvez, B.G. Importance and regulation of adult stem cell migration. *J. Cell. Mol. Med.* **2018**, *22*, 746–754. [CrossRef] [PubMed]

43. Liu, M.; Lei, H.; Dong, P.; Fu, X.; Yang, Z.; Yang, Y.; Ma, J.; Liu, X.; Cao, Y.; Xiao, R. Adipose-Derived Mesenchymal Stem Cells from the Elderly Exhibit Decreased Migration and Differentiation Abilities with Senescent Properties. *Cell Transplant.* **2017**, *26*, 1505–1519. [CrossRef] [PubMed]

44. Fu, X.; Liu, G.; Halim, A.; Ju, Y.; Luo, Q.; Song, G. Mesenchymal Stem Cell Migration and Tissue Repair. *Cells* **2019**, *8*, 784. [CrossRef] [PubMed]

45. Mishra, A.; Ojansivu, M.; Autio, R.; Vanhatupa, S.; Miettinen, S.; Massera, J. In-vitro dissolution characteristics and human adipose stem cell response to novel borophosphate glasses. *J. Biomed. Mater. Res. Part A* **2019**, *107*, 2099–2114. [CrossRef] [PubMed]

46. He, P.; Mann-Collura, O.; Fling, J.; Edara, N.; Hetz, R.; Razzaque, M.S. High phosphate actively induces cytotoxicity by rewiring pro-survival and pro-apoptotic signaling networks in HEK293 and HeLa cells. *FASEB J.* **2021**, *35*, e20997. [CrossRef] [PubMed]

47. Damaghi, M.; Wojtkowiak, J.; Gillies, R. pH sensing and regulation in cancer. *Front. Physiol.* **2013**, *4*, 70349. [CrossRef] [PubMed]

48. Barradas, A.M.C.; Monticone, V.; Hulsman, M.; Danoux, C.; Fernandes, H.; Birgani, Z.T.; Groot, F.B.-D.; Yuan, H.; Reinders, M.; Habibovic, P.; et al. Molecular mechanisms of biomaterial-driven osteogenic differentiation in human mesenchymal stromal cells. *Integr. Biol. Quant. Biosci. Nano Macro* **2013**, *5*, 920–931. [CrossRef]

49. Durand, L.A.H.; Góngora, A.; López, J.M.P.; Boccaccini, A.R.; Zago, M.P.; Baldi, A.; Gorustovich, A. In vitro endothelial cell response to ionic dissolution products from boron-doped bioactive glass in the SiO_2-CaO-P_2O_5-Na_2O system. *J. Mater. Chem. B* **2014**, *2*, 7620–7630. [CrossRef]

50. Lin, Y.; Brown, R.F.; Jung, S.B.; Day, D.E. Angiogenic effects of borate glass microfibers in a rodent model. *J. Biomed. Mater. Res. Part A* **2014**, *102*, 4491–4499. [CrossRef]

51. Durand, L.A.H.; Vargas, G.E.; Romero, N.M.; Vera-Mesones, R.; Porto-López, J.M.; Boccaccini, A.R.; Zago, M.P.; Baldi, A.; Gorustovich, A. Angiogenic effects of ionic dissolution products released from a boron-doped 45S5 bioactive glass. *J. Mater. Chem. B* **2015**, *3*, 1142–1148. [CrossRef]

52. Li, K.; Lu, X.; Razanau, I.; Wu, X.; Hu, T.; Liu, S.; Xie, Y.; Huang, L.; Zheng, X. The enhanced angiogenic responses to ionic dissolution products from a boron-incorporated calcium silicate coating. *Mater. Sci. Eng. C* **2019**, *101*, 513–520. [CrossRef] [PubMed]

53. Hazehara-Kunitomo, Y.; Hara, E.S.; Ono, M.; Aung, K.T.; Komi, K.; Pham, H.T.; Akiyama, K.; Okada, M.; Oohashi, T.; Matsumoto, T.; et al. Acidic Pre-Conditioning Enhances the Stem Cell Phenotype of Human Bone Marrow Stem/Progenitor Cells. *Int. J. Mol. Sci.* **2019**, *20*, 1097. [CrossRef] [PubMed]

54. Abdik, E.A.; Abdik, H.; Taşlı, P.N.; Deniz, A.A.H.; Şahin, F. Suppressive Role of Boron on Adipogenic Differentiation and Fat Deposition in Human Mesenchymal Stem Cells. *Biol. Trace Elem. Res.* **2019**, *188*, 384–392. [CrossRef] [PubMed]

55. Vuornos, K.; Ojansivu, M.; Koivisto, J.T.; Häkkänen, H.; Belay, B.; Montonen, T.; Huhtala, H.; Kääriäinen, M.; Hupa, L.; Kellomäki, M.; et al. Bioactive glass ions induce efficient osteogenic differentiation of human adipose stem cells encapsulated in gellan gum and collagen type I hydrogels. *Mater. Sci. Eng. C Mater. Biol. Appl.* **2019**, *99*, 905–918. [CrossRef] [PubMed]

56. Ojansivu, M.; Mishra, A.; Vanhatupa, S.; Juntunen, M.; Larionova, A.; Massera, J.; Miettinen, S. The effect of S53P4-based borosilicate glasses and glass dissolution products on the osteogenic commitment of human adipose stem cells. *PLoS ONE* **2018**, *13*, e0202740. [CrossRef] [PubMed]

57. Ojansivu, M.; Hyväri, L.; Kellomäki, M.; Hupa, L.; Vanhatupa, S.; Miettinen, S. Bioactive glass induced osteogenic differentiation of human adipose stem cells is dependent on cell attachment mechanism and mitogen-activated protein kinases. *Eur. Cells Mater.* **2018**, *35*, 54–72. [CrossRef] [PubMed]

58. Salgado, A.J.B.O.G.; Reis, R.L.G.; Sousa, N.J.C.; Gimble, J.M. Adipose tissue derived stem cells secretome: Soluble factors and their roles in regenerative medicine. *Curr. Stem Cell Res. Ther.* **2010**, *5*, 103–110. [CrossRef] [PubMed]

59. Ueno, M.; Lo, C.-W.; Barati, D.; Conrad, B.; Lin, T.; Kohno, Y.; Utsunomiya, T.; Zhang, N.; Maruyama, M.; Rhee, C.; et al. Interleukin-4 overexpressing mesenchymal stem cells within gelatin-based microribbon hydrogels enhance bone healing in a murine long bone critical-size defect model. *J. Biomed. Mater. Res. Part A* **2020**, *108*, 2240–2250. [CrossRef] [PubMed]

60. Zheng, K.; Fan, Y.; Torre, E.; Balasubramanian, P.; Taccardi, N.; Cassinelli, C.; Morra, M.; Iviglia, G.; Boccaccini, A.R. Incorporation of Boron in Mesoporous Bioactive Glass Nanoparticles Reduces Inflammatory Response and Delays Osteogenic Differentiation. *Part. Part. Syst. Charact.* **2020**, *37*, 2000054. [CrossRef]

61. Rahmati, M.; Mozafari, M. Selective Contribution of Bioactive Glasses to Molecular and Cellular Pathways. *ACS Biomater. Sci. Eng.* **2020**, *6*, 4–20. [CrossRef]

62. Angelova, M.I.; Bitbol, A.-F.; Seigneuret, M.; Staneva, G.; Kodama, A.; Sakuma, Y.; Kawakatsu, T.; Imai, M.; Puff, N. pH sensing by lipids in membranes: The fundamentals of pH-driven migration, polarization and deformations of lipid bilayer assemblies. *Biochim. Biophys. Acta BBA—Biomembr.* **2018**, *1860*, 2042–2063. [CrossRef] [PubMed]

63. Kim, N. pH variation impacts molecular pathways associated with somatic cell reprogramming and differentiation of pluripotent stem cells. *Reprod. Med. Biol.* **2020**, *20*, 20–26. [CrossRef] [PubMed]

64. Wei, D.; Engelman, D.M.; Reshetnyak, Y.K.; Andreev, O.A. Mapping pH at Cancer Cell Surfaces. *Mol. Imaging Biol.* **2019**, *21*, 1020. [CrossRef] [PubMed]

65. Anderson, M.; Moshnikova, A.; Engelman, D.M.; Reshetnyak, Y.K.; Andreev, O.A. Probe for the measurement of cell surface pH in vivo and ex vivo. *Proc. Natl. Acad. Sci. USA* **2016**, *113*, 8177–8181. [CrossRef] [PubMed]